Geomorphology 278 (2017) 149–162

Contents lists available at ScienceDirect

Geomorphology

journal homepage: www.elsevier.com/locate/geomorph

Prediction of spatially explicit rainfall intensity–duration thresholds for post-fire debris-flow generation in the western United States

Dennis M. Staley [a,*], Jacquelyn A. Negri [a], Jason W. Kean [a], Jayme L. Laber [b], Anne C. Tillery [c], Ann M. Youberg [d]

[a] U.S. Geological Survey, Golden, CO, USA
[b] National Weather Service, Los Angeles – Oxnard, CA, USA
[c] U.S. Geological Survey, Albuquerque, NM, USA
[d] Arizona Geological Survey, Tucson, AZ, USA

ARTICLE INFO

Article history:
Received 4 May 2016
Received in revised form 4 October 2016
Accepted 10 October 2016
Available online 14 October 2016

Keywords:
Wildfire
Debris flow
Rainfall thresholds
Hazard assessment

ABSTRACT

Early warning of post-fire debris-flow occurrence during intense rainfall has traditionally relied upon a library of regionally specific empirical rainfall intensity–duration thresholds. Development of this library and the calculation of rainfall intensity-duration thresholds often require several years of monitoring local rainfall and hydrologic response to rainstorms, a time-consuming approach where results are often only applicable to the specific region where data were collected. Here, we present a new, fully predictive approach that utilizes rainfall, hydrologic response, and readily available geospatial data to predict rainfall intensity–duration thresholds for debris-flow generation in recently burned locations in the western United States. Unlike the traditional approach to defining regional thresholds from historical data, the proposed methodology permits the direct calculation of rainfall intensity–duration thresholds for areas where no such data exist. The thresholds calculated by this method are demonstrated to provide predictions that are of similar accuracy, and in some cases outperform, previously published regional intensity–duration thresholds. The method also provides improved predictions of debris-flow likelihood, which can be incorporated into existing approaches for post-fire debris-flow hazard assessment. Our results also provide guidance for the operational expansion of post-fire debris-flow early warning systems in areas where empirically defined regional rainfall intensity–duration thresholds do not currently exist.

Published by Elsevier B.V.

1. Introduction

Over the past several decades, the frequency of large wildfires, length of fire season, and duration of individual wildfires have steadily increased in the western United States as a result of a combination of human activities, evolving land-use patterns, weather, and climate (Westerling et al., 2006). An increase in the susceptibility to debris flow is a secondary effect of wildfire in recently burned steeplands, a hazard which may persist for several years following fire containment (Cannon and DeGraff, 2009; Cannon et al., 2010; DeGraff et al., 2015). Risk associated with debris-flow hazards increases as populations expand into foothill and mountainous areas susceptible to wildfire. In addition, a greater incidence of fire activity in mountainous areas with relatively infrequent fire recurrence may increase the potential of debris flows in environments or communities where debris-flow hazard has been historically absent (Cannon and DeGraff, 2009). The geographic expansion of areas exposed to post-fire debris-flow hazard has motivated efforts to reduce exposure of people, infrastructure, and important natural, cultural, and economic resources to these hazards. Hazard assessment provides the first step in reducing public exposure to these events, as this process identifies areas vulnerable to post-fire debris-flow generation, and provides estimates of the magnitude of an event, should one occur (Cannon et al., 2008, 2010, 2011; Staley et al., 2013a, 2013b, 2013c).

In the western United States, the most common methods for post-fire debris-flow hazard assessment are based upon statistical models that predict the likelihood and magnitude of debris flow for a specific location using historical data (Gartner et al., 2008, 2014; Cannon et al., 2010). These hazard assessments (e.g. Cannon et al., 2009; Parise and Cannon, 2012; USGS, 2016) are useful for identifying and prioritizing areas of potential debris-flow hazard for planning purposes, but are not intended for direct predictive use in early warning systems (Cannon et al., 2010). Instead, post-fire debris-flow early warning in the western United States relies upon regionally specific rainfall intensity–duration thresholds (Cannon et al., 2008, 2011; Staley et al., 2013b, 2015). Regional thresholds are determined from historical data that characterize the rainfall intensities that produced, or did not produce, debris flows for specific locations. The empirical approach for establishing regional rainfall intensity–duration thresholds requires an extensive library of rainfall and basin response information from which the thresholds can be calculated by either subjective (e.g.

* Corresponding author at: Box 25046 MS966 DFC, Denver, CO 80225, USA.
E-mail address: dstaley@usgs.gov (D.M. Staley).

http://dx.doi.org/10.1016/j.geomorph.2016.10.019
0169-555X/Published by Elsevier B.V.

Cannon et al., 2008, 2011) or objective methods (Staley et al., 2013b, 2015).

Empirically derived rainfall intensity–duration thresholds for the generation of runoff-induced post-fire debris-flows in southern California (Cannon et al., 2008, 2011; Staley et al., 2013b) compose a major component of the U.S. Geological Survey (USGS) and the National Oceanic and Atmospheric Administration (NOAA) post-fire debris-flow early warning system, currently operating in the National Weather Service (NWS) Los Angeles–Oxnard and San Diego weather forecasting offices (NOAA, 2005). Intensive research and monitoring over a span of >10 years was needed to define regional thresholds sufficiently robust for inclusion in a warning system. This system involved the comparison of forecasted and real-time estimates of rainfall intensity to preexisting intensity–duration thresholds. How closely the forecasted or observed rainfall rates compare to the threshold values are a major factor in the decision-making process for issuing debris-flow outlooks, watches, and warnings (USGS, 2005). The success of the early warning system in southern California has resulted in significant interest in the expansion of the program to other fire-prone regions of the United States; however, expansion using the current framework is hampered by time-consuming development of regional rainfall thresholds.

In an effort to expand operational capabilities to areas with no established regional intensity–duration thresholds, we develop and test a new framework that integrates statistical methods of characterizing debris-flow susceptibility with empirical methods for determining rainfall intensity–duration thresholds. Specifically, our new framework combines approaches for calculating the statistical likelihood of post-fire debris flows using logistic regression with objective techniques for defining rainfall intensity–duration thresholds. The combination provides a single method that can (1) predict the likelihood that a debris flow will occur at a given rainfall intensity, and (2) define accurate, spatially explicit rainfall thresholds, which correspond to the rainfall intensity that results in a 50% likelihood of debris flow.

2. Post-fire debris-flow hazard prediction

The prediction of runoff-induced post-fire debris-flow occurrence has traditionally relied upon statistical methods that calculate a likelihood of debris-flow generation in response to rainfall of a given intensity using logistic regression (Rupert et al., 2008; Cannon et al., 2010) and the identification of rainfall rates that correspond to increased probability of debris-flow occurrence during a rainstorm using empirical rainfall intensity-duration thresholds (Cannon et al., 2008, 2011; Staley et al., 2013b, 2015). To date (September 2016), these methods have remained independent. Here, we review existing methods for the prediction of debris-flow likelihood and the calculation of rainfall intensity–duration thresholds for debris-flow generation in recently burned watersheds; then we describe methods for the integration of these two approaches.

2.1. Debris-flow likelihood

Logistic regression models are frequently used to predict the likelihood of post-fire debris flows (e.g. Cannon et al., 2009, 2010; Staley et al., 2013a, 2013c, 2016; Staley, 2014, Nyman et al., 2015; USGS, 2016). This approach utilizes the logistic curve to define the statistical likelihood of a binary response (i.e. debris-flow generation) as:

$$P = \frac{e^x}{1 + e^x} \tag{1}$$

where P is a number ranging from 0 to 1 and represents the statistical likelihood of debris-flow occurrence (where values approaching 1 indicate an increasing likelihood) and χ is determined by the link function:

$$\chi = \beta + C_1X_1 + C_2X_2 + \ldots + C_nX_n \tag{2}$$

where β and C_1, C_2, …,C_n are empirically derived parameters and X_1, X_2, …,X_n represent independent variables that influence the occurrence of the event.

Cannon et al. (2010) detailed the methods used to calculate the statistical likelihood of post-fire debris-flow occurrence in the intermountain western United States using logistic regression (Table 1). This technique incorporated data of past debris-flow occurrence combined with rainfall intensity data, and geospatial data characterizing basin morphometry, burn severity, and soil properties to calculate the likelihood that a post-fire debris flow will occur given a rainfall intensity associated with a rainstorm of a known recurrence interval. Staley et al. (2013a), using the methods and data from Rupert et al. (2008) and Cannon et al. (2010), developed the most recent model of statistical likelihood used for debris-flow hazard assessment in southern California (USGS, 2016).

The logistic regression approach to predicting post-fire debris-flow likelihood is advantageous as it is computationally simple, utilizes free, readily available geospatial data, and provides a statistical likelihood of the occurrence of debris flows for storms of different magnitudes in geospatial format at the scale of a stream segment or drainage basin (e.g. Tillery et al., 2012; Verdin et al., 2012; USGS, 2016). The link function parameter values (Eq. (2)) for the predictive models of post-fire debris-flow generation in the western United States are displayed in Table 1.

2.2. Rainfall intensity–duration thresholds

Rainfall intensity–duration thresholds are empirical models that represent the nonlinear increase in the likelihood of a post-fire debris flow at or above a given rainfall intensity, and are typically portrayed in the form of a power-law equation (Caine, 1980; Schumm, 1980). The actual value of the threshold represents the rainfall intensity (as measured over a given duration), below which there is a lower probability of debris-flow initiation, and above which there is a rapid increase in the likelihood of initiation. Rainfall thresholds are commonly used for the prediction of landslides and debris flows throughout the world (Godt et al., 2006; Guzzetti et al., 2007, 2008; Godt and McKenna, 2008; Brunetti et al., 2010).

Cannon et al. (2008) developed the first post-fire debris-flow threshold equations for the western United States. These thresholds were defined by visually placing single intensity–duration thresholds at the lower limit of the peak rainstorm intensities that had produced post-fire debris flows, and at the upper limit of peak rainstorm intensities that do not produce post-fire debris flows. Staley et al. (2013b) refined the method developed by Cannon et al. (2008) for recently burned watersheds in the San Gabriel and Santa Ana Mountains by proposing a method that more objectively defined the intensity–duration threshold by minimizing incorrect predictions through the numerical balancing of false alarms (above threshold, no debris-flow occurrence) and failed alarms (below threshold, debris-flow occurrence). The approach of Staley et al. (2013b) also differed from previous studies in that it incorporated triggering rainfall intensities, which the authors defined as the highest rainfall intensity recorded immediately prior to the passage of a post-fire debris flow at a monitoring location.

Rainfall thresholds have been identified for several physiographic regions in the western United States using both subjective methods based on the peak rainfall intensities for an observed rainstorm (Cannon et al., 2008, 2011), and objective methods based on measured triggering rainfall intensity (Staley et al., 2013b, 2015; Youberg, 2014). Since triggering intensities are difficult to precisely define because debris-flow timing is often unknown, only thresholds defined from peak rainstorm intensities are currently available for most of the western United States (Table 2).

Table 1
Previously published logistic regression link functions for predicting the statistical likelihood of post-fire debris-flow generation in the western United States.

Model region	Intermountain Western United States (A)	Intermountain Western United States (B)	Southern California (1)	Southern California
Source	Cannon et al. (2010)	Cannon et al. (2010)	Rupert et al. (2008)	USGS (2016)
β	−0.7	−7.6	−20.807	−5.22
C_1	0.03	−1.1	1.65	0.003
X_1	Percentage of basin area with gradients ≥30%	Ruggedness	ln(Relief), in m	Relief, in m
C_2	−1.6	0.06	−0.694	0.008
X_2	Ruggedness	Percentage of basin area burned at high or moderate severity	ln(Average channel length), in km	Percentage of basin area burned at high or moderate severity and gradients ≥50%
C_3	0.06	0.09	2.463	0.024
X_3	Percentage of basin area burned at high or moderate severity	Soil clay content, in %	Peak 3-h storm intensity, in mm h^{-1}	Average gradient of burned terrain, in %
C_4	0.2	−1.4	0.128	−0.007
X_4	Soil clay content, in %	Soil organic matter, in %	Soil slope, in %	Soil clay content, in %
C_5	−0.4	0.06	7.229	0.105
X_5	Soil liquid Limit	Average storm intensity, in mm h^{-1}	Soil organic matter, in %	Peak 30-min storm intensity, in mm h^{-1}
C_6	0.07	-	−0.245	-
X_6	Average storm intensity, in mm h^{-1}	-	Soil clay content, in %	-

2.3. Relation between debris-flow likelihood and rainfall thresholds

To date, the predictions based on regional intensity–duration thresholds and predictive models of post-fire debris-flow likelihood remain independent, and are often inconsistent. Regional thresholds provide a single threshold value per measured duration, and do not characterize the spatial variability identified during hazard assessment. For example, the regional 15-min rainfall intensity–duration threshold for the San Gabriel Mountains has been determined to be 18.6 mm h^{-1} (Staley et al., 2013b). However, this single value fails to account for variations in topography, burn severity, and soil properties that may influence the actual rainfall rates needed to generate debris flows in a specific watershed. Therefore, a need exists to develop a method that can be used to determine a spatially explicit (i.e. site-specific) rainfall intensity–duration threshold that characterizes the variability of debris-flow hazard in different locations.

Hazard assessments based on logistic regression were originally designed solely to identify areas susceptible to debris flows. The approach can also, in principle, be inverted to define rainfall thresholds. For example, a rainfall intensity–duration threshold for a recently burned basin could be defined as the rainfall rate at which the statistical likelihood of debris flow exceeds $p = 0.5$. Despite the link between debris-flow probability and rainfall thresholds, the structure of the current probability equations is not suitable for defining realistic rainfall thresholds. In the current predictive models, rainfall variables influence the link function independently of the variables associated with topography, burn severity or soil properties. As such, values of $P > 0$ occur in the existing likelihood equations (Cannon et al., 2010; USGS, 2016) even when it is not raining. For example, using the Cannon et al. (2010) Intermountain West model A (Table 1) for a recently burned basin with the variable values equal to the following: percent slope ≥30% = 91.2%; ruggedness = 0.55, percent burned at high or moderate severity = 100%, clay content = 30.7% and liquid limit = 32.5, it would require rainfall intensity = −0.43 mm h^{-1} for $P = 0.5$. Since this model predicts a negative rainfall intensity in order to achieve $P = 0.5$, it is impractical to use the logistic regression models in their current form to predict spatially explicit rainfall intensity–duration thresholds. For this reason, the NOAA/USGS early warning system still relies upon the regional rainfall intensity–duration thresholds based upon a library of historical data rather than the current probabilistic models of post-fire debris-flow generation, which precludes the expansion of this system into areas where no such data exist. In the remainder of this paper, we will show how the approaches for estimating debris-flow probability and defining rainfall intensity thresholds can be merged. The approach is demonstrated to define accurate, basin-specific rainfall intensity thresholds across the western U.S., even in areas not included in the dataset used to calibrate the model.

3. Conceptual model of post-fire debris-flow generation and likelihood

Previously, logistic regression models of post-fire debris-flow generation (e.g. Rupert et al., 2008; Cannon et al., 2010) relied upon a stepwise statistical approach for variable selection. Model success was

Table 2
Regional rainfall intensity–duration thresholds for post-fire debris-flow occurrence in the western United States. The training dataset was used to calibrate the logistic regression parameters, while the test dataset was used to evaluate the predictive success of the calibrated models.

Threshold region	State	Dataset	Source	15-min Threshold (mm h^{-1})	30-min Threshold (mm h^{-1})	60-min Threshold (mm h^{-1})
Ventura and Santa Barbara Counties, California (VEN)	California	Training	Cannon et al. (2008)	21.8	16.3	12.4
San Gabriel, San Bernardino and San Jacinto, Santa Ana Mountains, California (SGSBSJ)	California	Training	Staley et al. (2013b)	18.6	12.7	11.7
Orange and San Diego Counties, California (OSD)	California	Training	This Study	30.5	20.3	12.7
Central New Mexico (CNM)	New Mexico	Test	This Study	27.4	17.8	12.8
Northern Arizona (NAZ)	Arizona	Test	Youberg (2014)	62.0	52.0	33.0
Southern Arizona (SAZ)	Arizona	Test	Youberg (2014)	43.0	24.0	14.0
Western Colorado (WCO)	Colorado	Test	Cannon et al. (2008)	17.2	10.6	6.5
Southwestern Colorado (SWCO)	Colorado	Test	Cannon et al. (2008)	25.1	15.4	9.5
Colorado Front Range (FRCO)	Colorado	Test	Staley et al. (2015)	30.6	18.8	11.6
Southwestern Montana (SWMT)	Montana	Test	This Study	39.6	25.3	12.9

measured solely upon statistical performance. While this approach provided an objective, non-biased method for variable selection and evaluation of model performance, the physical relevance of the variables and their effects on model predictions of likelihood were sometimes counterintuitive or in conflict with more recent field observations and measurements of post-fire debris-flow generation.

A number of field and laboratory studies concerning post-fire debris-flow generation have been conducted (e.g. Kean et al., 2011, 2012; Lamb et al., 2011; Schmidt et al., 2011; Smith et al., 2012; Staley et al., 2013b, 2014) since the original logistic regression models were published by Rupert et al. (2008) and Cannon et al. (2010). The insights gained from these field studies provide useful data for the development of a simple conceptual model of the factors that influence the likelihood of debris-flow initiation by runoff-induced progressive sediment bulking processes in a recently burned watershed (Cannon, 2001; Cannon et al., 2003). Here, we propose the following conceptual model of post-fire debris-flow likelihood used to develop the logistic link function χ:

$$\chi = f(T, F, S, R) \tag{3}$$

where T is a metric characterizing terrain steepness, F is a metric characterizing the intensity of wildfire, S is a measure of surface properties that influence sediment availability or erodibility, and R is a metric characterizing the intensity of rainfall.

Terrain steepness has been found to directly influence the rates of hillslope and channel erosion, and the stability of hillslope and channel sediment, which — individually or collectively — contributes to the transition of surface runoff to debris flow in recently burned areas (Gabet, 2003a, 2003b, 2003c; Kean et al., 2011, 2013; Lamb et al., 2011, 2013; Nyman et al., 2011; Schmidt et al., 2011; Smith et al., 2012; Prancevic et al., 2014; Staley et al., 2014). Terrain steepness also influences the efficacy of gravitational and runoff-related erosion and sediment transport processes on hillslopes and in stream channels, all of which contribute to an increase in the availability of sediment for post-fire debris-flow initiation. Sediment transport rates from gravitational processes, such as rockfall and dry ravel, tend to be significantly higher following wildfire, with the highest rates found on steep slopes (Florsheim et al., 1991, 2016; Gabet, 2003c; Lamb et al., 2011, 2013). Slope gradient also directly influences the shear stress of overland, rill, and channelized flow processes, and the erosion of hillslope and channel materials by runoff has been recognized as a significant source of material in post-fire debris flows (Cannon, 2001; Cannon et al., 2003; Santi et al., 2008; Schmidt et al., 2011; Parise and Cannon, 2012; Smith et al., 2012; Staley et al., 2014).

The intensity and duration of wildfire directly relate to reductions in protective cover and changes in the physical and chemical properties of soils, thereby elevating the runoff response during rainfall and increasing the susceptibility of the surface to erosion processes. Increased runoff, when combined with steep slopes and readily available sediment, has long been recognized as the primary ingredient for post-fire debris flow initiation (Chawner, 1935; Eaton, 1935; Rowe et al., 1949; Hamilton et al., 1954; Parrett, 1987; Wells, 1987; Meyer and Wells, 1997; Cannon, 2001). Combustion of the vegetation canopy and litter decreases interception, resulting in an increased amount of rainfall directly impacting the ground surface, and an enhanced vulnerability to raindrop-impact-induced erosion processes (Moody and Martin, 2001; Kinnell, 2005; Shakesby and Doerr, 2006; Larsen et al., 2009). The combustion of vegetation during fire may also result in the development of an ash crust and the infiltration of ash into the soil column, effectively blocking pore space and reducing infiltration capacity (Balfour et al., 2014; Bodí et al., 2014), although the effects of ash may be spatially variable and short lived (Larsen et al., 2009). Of particular concern is the creation or enhancement of hydrophobicity in the top few centimeters of soil (DeBano, 2000). Volatilization of water-repellent organic compounds in soils and near-surface vegetation may bond with mineral soil particles, reducing the ability of the soil to absorb moisture (DeBano, 2000; Letey, 2001). Other physical changes to the soil have been associated with wildfire, including hyper-dry conditions (Moody and Ebel, 2012), a decrease in saturated hydraulic conductivity (Ebel and Moody, 2013), surface sealing by detached soil particles (Larsen et al., 2009), and a decrease in structural and particle cohesion and corresponding decrease in critical shear stress (Giovannini and Lucchesi, 1983; Giovannini et al., 1987; Moody et al., 2005; Wagenbrenner et al., 2010; Al-Hamdan et al., 2012; Nyman et al., 2013). All these serve to decrease infiltration rates and increase the erodibility of fire-affected soils. Positive interaction between these physical and chemical changes in soil properties and the enhanced post-fire hydrologic response results in an increase in sediment availability and transport rates in recently burned areas (Moody et al., 2013).

Surface properties relate to debris-flow susceptibility by influencing infiltration capacity, erodibility (shear strength), and sediment availability. Soils with lower infiltration capacities are inherently more susceptible to runoff and debris-flow generation during intense rainfall (Noske et al., 2016). However, the influence of fire on post-fire infiltration rates often varies with soil type, vegetation, and the severity of wildfire (Martin and Moody, 2001). Soil erodibility is a function of shear strength, where soils with less shear strength are likely to have higher rates of sediment transport (Moody et al., 2005; Nyman et al., 2013). Finally, debris-flow generation is dependent upon availability of sediment, where transport limited watersheds are more likely to generate debris flows than supply-limited basins (Bovis and Jakob, 1999).

The occurrence of post-fire debris flows has also been found to be linked with pulses of high-intensity rainfall and the generation of runoff from infiltration-excess (Hortonian) overland flow (Wells, 1987; Gabet, 2003a; Cannon et al., 2008; Kean et al., 2011; Staley et al., 2013b), which occurs when rainfall rates exceed the infiltration capacity of the soil (Ebel and Moody, 2013; Moody and Ebel, 2014). Antecedent moisture conditions (e.g. after wildfire, within storm or seasonal) have been found to have very little, if any, influence on the likelihood of post-fire debris-flow initiation (Cannon et al., 2008). In a plot-scale field experiment, Wells (1987) was able to initiate small debris flows after only 3 min of rainfall at intensities between 12 and 55 mm h^{-1}. Several papers documented the occurrence of post-fire debris flow after 16 min of moderate intensity rainfall during the very first rainstorm (when soil moisture content was extremely low) following wildfire in a recently burned watershed in the San Gabriel Mountains (Kean and Staley, 2011; Kean et al., 2011; Schmidt et al., 2011; Staley et al., 2013b). From precise monitoring of debris-flow timing, Kean et al. (2011) identified a near-zero lag time between the occurrence of short bursts of high-intensity rainfall and the passage of a debris flow at the monitoring site. The best temporal correlation and shortest lag between rainfall intensity and debris-flow initiation was identified for rainfall intensity measured between 5 and 30 min durations (Kean et al., 2011, 2012; Staley et al., 2013b). In addition, the first flow in a stream channel below a burn area (as measured by flow stage) is frequently the passage of a debris flow (Kean and Staley, 2011; Kean et al., 2011, 2012).

4. Methodology

This study relied upon the established methods of logistic regression (Eqs. (1) and (2)) and receiver operating characteristics (ROC) analysis (Swets, 1988; Fawcett, 2006) to develop a new method for the spatially explicit prediction of rainfall intensity-duration thresholds. Logistic regression models were based upon empirical data collected within the first two years of wildfire in recently burned areas in the western United States (Fig. 1 and Table 3). In total, the database used for this study consisted of 1550 records, and included information pertaining to location, hydrologic response (debris flow or no debris flow), rainfall rates, surface properties, and the morphological properties of the contributing area (Staley et al., 2016). The area of drainage basins included in the database ranged between 0.02 and 8 km^2.

4.1. Debris-flow database

Rainfall data were collected at nearby (maximum distance = 4 km) rain gages from a variety of sources, including USGS, NOAA, and other state, county, and local agencies. Selected rain gages were situated at similar elevation and slope aspect as the monitoring locations. A maximum distance of 4 km was selected as it represented a balance between number of database records and the representativeness of the recorded

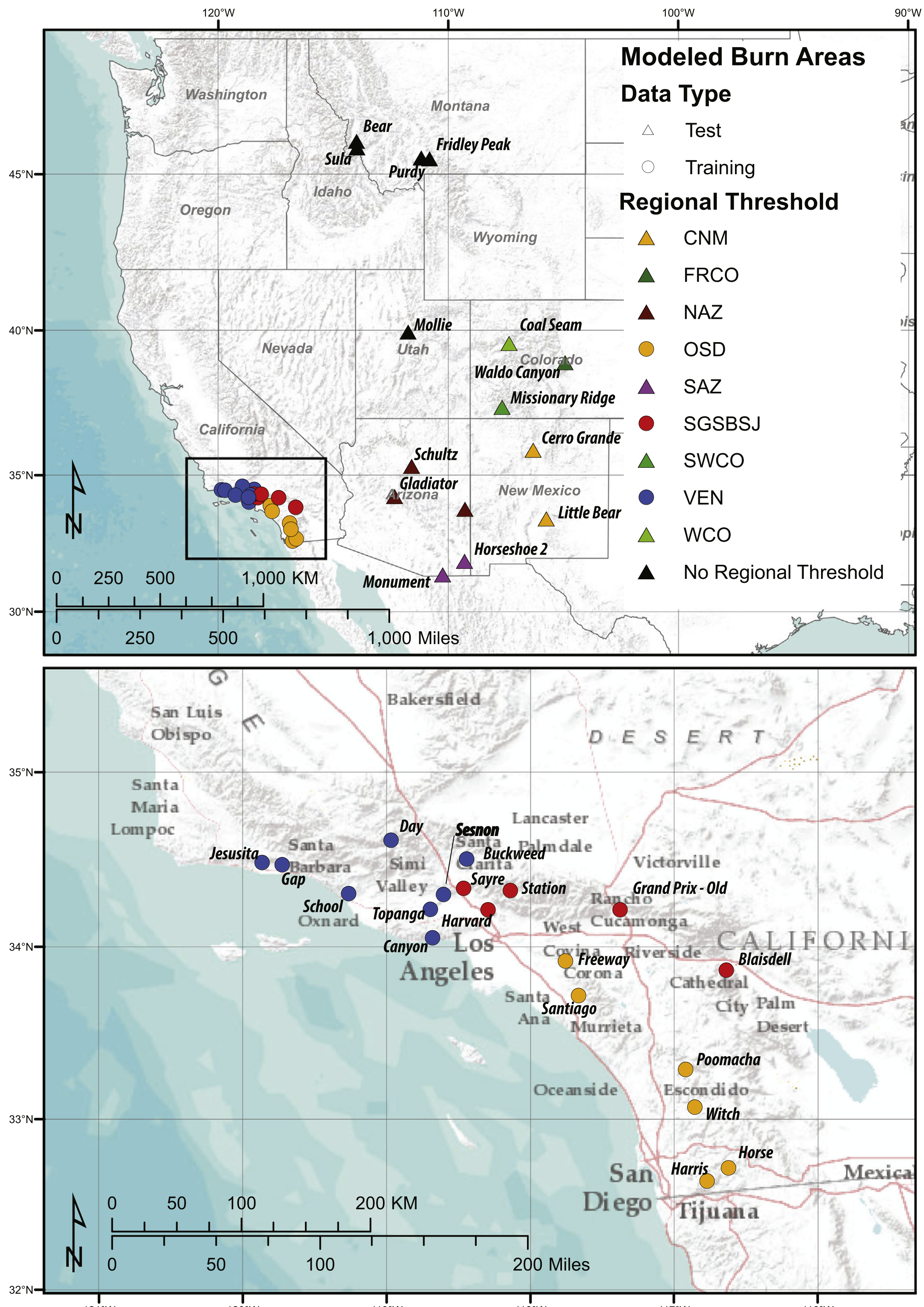

Fig. 1. Overview map displaying burn areas included in training dataset (triangles) and test database (circles) and threshold regions (see Table 2 for additional regional threshold information).

Table 3
Fires, number of records, and number of debris flows for data included in training and test datasets. State column represents U.S. State abbreviations [AZ = Arizona, CA = California, CO = Colorado, MT = Montana, NM = New Mexico, UT = Utah]. Threshold region represents the abbreviation for regional thresholds defined in Table 2.

Training data

Fire name	Abbreviation	State	Year	N records	N debris flows	Threshold region
Buckweed	bck	CA	2007	16	0	VEN
Blaisdell	bla	CA	2005	10	0	SGSBSJ
Canyon	can	CA	2007	14	0	VEN
Day	day	CA	2006	8	0	VEN
Freeway	fwy	CA	2008	8	0	OSD
Gap	gap	CA	2008	10	0	VEN
Grand Prix - Old	gpo	CA	2003	78	60	SGSBSJ
Harris	har	CA	2007	10	0	OSD
Horse	hrs	CA	2006	9	0	OSD
Harvard	hrv	CA	2005	28	6	SGSBSJ
Jesusita	jes	CA	2009	6	0	VEN
Poomacha	poo	CA	2007	21	19	OSD
Santiago	san	CA	2007	12	5	OSD
Sayer	say	CA	2008	14	2	SGSBSJ
School	sch	CA	2005	12	0	VEN
Sesnon	ses	CA	2008	4	0	VEN
Station	stn	CA	2009	600	108	SGSBSJ
Topanga	top	CA	2005	33	0	VEN
Witch	wit	CA	2007	46	1	OSD

Test data

Fire name	Abbreviation	State	Year	N records	N debris flows	Threshold region
Bear	br	MT	2000	14	11	-
Cerro Grande	cg	NM	2000	11	5	CNM
Coal Seam	cs	CO	2002	253	17	WCO
Fridley Peak	fri	MT	2001	11	5	-
Gladiator	gld	AZ	2012	35	3	NAZ
Horseshoe 2***	h2f	AZ	2011	30	4	SAZ
Little Bear	lb	NM	2012	47	30	CNM
Monument	mmt	AZ	2011	19	6	SAZ
Mollie	mol	UT	2001	4	4	-
Missionary Ridge	mr	CO	2002	16	11	SWCO
Purdy	pur	MT	2001	9	0	-
Schultz***	scz	AZ	2010	105	26	NAZ
Sula	sul	MT	2000	6	2	-
Waldo Canyon	wal	CO	2012	31	7	FRCO
Wallow	wlw	AZ	2011	20	2	NAZ

*** Differenced normalized burn ratio not available.

intensities for characterizing the spatially variable rainfall rates that characterize convective storms in the western United States. For this study, individual storms were defined by a minimum of 8 h without rainfall. Hydrologic response information was collected by USGS personnel and local collaborators.

The variables used to characterize the contributing area for each record were derived from publicly available geospatial data sources. While higher-resolution data sources may be available for specific locations, we chose to use the following data sources because they are available nationwide, and allow for consistent calculation of metrics for any burn area in the United States. Topographic data were derived from 10-m digital elevation models (USGS, 2015) and surface property data were extracted from the STATSGO database (Schwartz and Alexander, 1995). Differenced normalized burn ratio (dNBR) data were obtained from the Monitoring Trends in Burn Severity website (Eidenshink et al., 2007). Burn severity information was provided by local Burned Area Emergency Response (BAER) teams, who field-validated Burned Area Reflectance Classification (BARC) imagery derived from the dNBR data (Key and Benson, 2006).

We split the debris-flow database into two datasets for model calibration and evaluation. The training dataset was used to calibrate the model parameters, and consisted of 939 records in southern California, of which 201 were from debris-flow producing rainstorms. The test dataset was used to evaluate the predictive performance of the calibrated model, and consisted of 611 total records (133 debris-flow events) from other areas in the western United States. While other methods of model calibration and validation were also evaluated (e.g. randomly split datasets using 75% of the records, and bootstrapping with 1000 iterations using 75% of the records), we divided the dataset in this manner for three reasons. First, the data included in the training dataset were collected as a part of a broader USGS Landslide Hazards Program monitoring effort in southern California. We consider these data to be of the highest quality with regards to rain gage accuracy, proper identification of hydrologic response, and location of response. Data included in the test dataset were also of high quality and were checked for accuracy, but different data sources (e.g. different types of rain gages, different observers of hydrologic response) may have resulted in slight inconsistencies in rainfall and response characterization. Second, the training and test datasets had similar ranges in variable values for the proposed model (Staley et al., 2016). We consider the data included in the training dataset to be representative of the range of variable values found in the test dataset. Finally, this method of geographic division of the data provided the greatest degree of model accuracy on both training and test datasets, as measured by regression evaluation statistics and model classification evaluation methods.

4.2. Model development

The training dataset was then used to develop a model of statistical likelihood of debris-flow occurrence and define rainfall intensity–duration thresholds for debris-flow generation using logistic regression methods. Hereafter, the term "logistic model" refers to the set of equations used to predict threshold rainfall intensities at multiple durations. Each logistic model comprised multiple equations with identical variables and differing parameter values for R, the rainfall accumulation totals (in mm) over multiple durations. To determine the logistic models with the greatest predictive capability, we iterated through multiple combinations of variables using the conceptual model (Eq. (3)) as a template for variable selection.

Based on our conceptual model, a realistic prediction of debris-flow generation requires that post-fire debris-flow likelihood should be close to zero in the absence of rainfall. This can be accomplished through the multiplicative combination of rainfall accumulation with variables related to basin morphology, fire severity and soil properties, such that the link function for the new logistic model follows the equation:

$$\chi = \beta + C_1TR + C_2FR + C_3SR \tag{4}$$

where C_1, C_2, and C_3 are empirically defined coefficients; and R is in mm measured over a given duration (in this case, we used durations of 15, 30, 60, 180 and 360 min). This link function can then be used to calculate the statistical likelihood of occurrence using Eq. (1). When $R = 0$ mm, the statistical likelihood is dependent solely upon the value of the intercept (β in Eq. (2)), where the value of P will asymptotically approach zero with increasingly negative values of β.

Once the model parameters in Eq. (4) have been calibrated using the training data and traditional logistic regression methods, the model can be used to solve for R at a given value of P (R_p) when C_1T, C_2F, and $C_3S > 0$, such that:

$$R_P = \frac{\ln\left(\frac{p}{1-p}\right) - \beta}{C_1T + C_2F + C_3S} \tag{5}$$

Because R in Eqs. (4) and (5) represents rainfall accumulation (in mm) over a fixed duration (e.g. 15, 30, and 60 min), and rainfall thresholds for post-fire debris-flows are most frequently reported as intensities in mm h^{-1} (e.g. Cannon et al., 2008, 2011; Staley et al., 2013b, 2015), we converted accumulation values of R_P to intensities using the equation:

$$I_p = \frac{R_P}{D} \tag{6}$$

where I_P is rainfall intensity (in mm h^{-1}) that results in a given likelihood, and D is the duration over which rainfall intensity was measured, in hours. For the purposes of this paper, we consider I_p that result in $p = 0.5$ as equivalent to a rainfall intensity–duration threshold. It should be noted that this approach permits the use of different values of p depending upon the application (e.g. a lower value of p might be used for a more conservative threshold, such as for a watershed immediately upstream of large, at-risk populations such as those that might be found at a school, hospital, or campground). Using Eqs. (5) and (6), we were able to calculate the rainfall intensity–duration thresholds for durations of 15, 30, and 60 min for each record in the training and test datasets. Note that the separate sets of coefficients C_1, C_2, and C_3 are determined for each duration in the analysis.

4.3. Model evaluation

Once the logistic models and rainfall intensity–duration thresholds for all possible variable combinations were calculated, we employed a semi-objective method for selection of the final logistic models (Negri, 2016). Logistic model performance was evaluated using (1) statistical measures of logistic regression, (2) objective measures of logistic model performance derived from ROC analysis, (3) the sensitivity of the model to minor changes in the values of the independent variables, and (4) the ability of the equation to reflect our conceptual understanding of the factors that influence post-fire debris-flow generation in the western United States.

The number of logistic models was initially reduced using statistical and objective performance metrics calculated on the training dataset. First, only logistic models where all coefficients and variables were statistically significant ($\alpha = 0.90$) for the analyzed durations were selected. Second, the statistical performance of each logistic model was compared using Akaike Information Criterion (*AIC*) (Akaike, 1974). *AIC* is a metric that characterizes both predictive performance and model complexity, where smaller *AIC* values reflect better model performance when the number of parameters and total number of records are equal. To insure physically realistic (i.e. positive) values of R in Eq. (4), only logistic models with positive coefficients C_1, C_2, and C_3 were selected for further inclusion. In the cases of variables with negative coefficients such as saturated hydraulic conductivity and clay content, the inverse value of the variable was calculated in order to meet the requirement of positive coefficient values.

Once the number of potential logistic models was reduced using statistical information based on the training dataset, model performance was evaluated on the test dataset using ROC methods (Swets, 1988; Fawcett, 2006). ROC methods have been used to assess the performance of landslide susceptibility models and to objectively define rainfall intensity–duration thresholds for post-fire floods and debris flows (Carrara et al., 2008; Godt et al., 2008; Frattini et al., 2009; Baum et al., 2010; Cervi et al., 2010; Staley et al., 2013b, 2015; Nyman et al., 2015). We tested the predictive accuracy of the logistic models by comparing the predicted threshold intensities and regional thresholds (Table 2) to known responses at locations in the test dataset. The literature contains seven published regional thresholds for post-fire debris-flow generation in the western United States (Cannon et al., 2008; Staley et al., 2013b, 2015; Youberg, 2014). For two areas where there are no published thresholds but sufficient data were available for threshold calculation, we employed objective methods (Staley et al., 2013b, 2015) to define three new regional thresholds: central New Mexico, Montana, and Orange and San Diego Counties, California. Data supporting the threshold calculations can be found in the appendix of Staley et al. (2016).

The spatially explicit rainfall intensity–duration threshold based on Eq. (5) was defined at the rainfall intensity (I_p in Eq. (6)) where $P = 0.5$, thereby converting the logistic regression model predictions of statistical likelihood to a binary classifier model. In this manner, there are four possible outcomes dependent upon event occurrence and model prediction. Event occurrence was considered to be either True or False (it either occurred or did not occur), while model predictions are considered to be Positive or Negative (successful prediction or prediction failure). The relationship between model prediction and event occurrence was then assigned to one of four classes. A true positive (*TP*) represented an event where rainfall rates exceeded threshold, and a debris flow was recorded. A true negative (*TN*) represented an event where rainfall rates were below critical threshold and no debris flows were recorded. False positive (*FP*) events occurred when rainfall rates exceeded threshold but no debris flows were triggered. This can also be considered a “false alarm” or type I error. A false negative (*FN*) occurs where rainfall rates were below threshold, yet a debris flow was recorded. This represents a “failed alarm” situation or type II error.

The ROC threat score metric was used to quantitatively describe the performance of each logistic model. Threat score represents a measure of the overall performance of the classifier model where a perfect model score would equal one, and each incorrect prediction (*FP* or *FN*) reduces the value of threat score (Schaefer, 1990). The threat score (*TS*) is calculated as:

$$TS = \frac{TP}{TP + FP + FN} \tag{7}$$

We chose to use *TS* because it equally weights the reduction in score for both *FN* and *FP* events, while not biasing the results based on the large number of *TN* records in the database.

Model sensitivity was evaluated using the standard deviation method of Friedman and Santi (2014). Here, the mean value of each variable was assigned for three of the four independent variables (e.g. T, F, S and R). We then evaluated the sensitivity of the model to the remaining variable by iteratively calculating P in 0.1 standard deviation increments. Models that displayed a high degree of sensitivity (i.e. more sensitive to changes in the analyzed variable than to rainfall intensity) to minor changes in variable values were excluded from further analyses.

Subjective methods were also employed to further reduce the number of potential logistic models, as expert-driven selection of model variables is an accepted and important component of logistic regression model development (Hosmer et al., 2000). The logistic models selected for further inclusion contained coefficients and variables that represent physically relevant ground conditions that have been demonstrated to contribute to elevated post-fire debris-flow hazard. Although logistic models that contained certain variables may have met the objective conditions outlined above, the physical relevance of those variables was not always easily explained. For example, logistic models that suggested a positive coefficient with soil permeability (related to saturated hydraulic conductivity and infiltration rate) were excluded from further consideration, as runoff generation is a primary mechanism for debris-flow initiation (Cannon, 2001; Kean et al., 2011).

5. Results and discussion

Our selection criteria outlined above resulted in the identification of four potential logistic models (M1, M2, M3 and M4). Variables, intercept values, and coefficient values for each model are listed in Table 4. Statistical and ROC performance measures for the training and test datasets, and existing regional thresholds, are reported in Table 5.

In the following sections we discuss (1) the results of the model calibration and evaluation of sensitivity based on the training dataset, (2) the performance of the selected logistic models as compared to nine regional intensity–duration thresholds (Table 2) throughout the western United States, (3) a case study of model results for two canyons in the Waldo Canyon burn area, Colorado, both of which experienced significant debris flows during the summer of 2013, and (4) a case study of the within-storm rainfall rates during the 6 February 2010 debris-flow producing rainstorm in Mullally Canyon, Station burn area, Los Angeles County, California. The two case studies provide examples of the spatially explicit application of the model predictions for site-specific analysis of seasonal and within-storm debris-flow likelihood calculation.

5.1. Model variables and sensitivity

Four measures of terrain steepness are represented in the final models (Table 4): the proportion of upslope area burned at high or moderate severity with gradients ≥23° (M1), the average gradient (sine) of the upslope area burned at high or moderate severity (M2), ruggedness, which is the relief of the upslope area divided by the total upslope area, in square meters (M3), and the proportion of upslope area burned with gradients ≥30° (M4). While it would be ideal for the model to consider topography completely separate from any measure of burn severity (e.g. high and moderate severity areas are combined with measures of gradient in M1 and M2), the statistical performance of the combined metrics yielded quantitatively better predictions, and are therefore included here. The slope values contained in M1 (23°) and M4 (30°) represent threshold slopes obtained by iteratively assessing the statistical performance of several potential threshold values (17°, 23°, 30°, and 45°). The variables that quantify the gradients or proportions of the different burn severities (M1, M2, and M3) characterize the influence of steep slopes in the contributing area that have elevated erosion and runoff potential. Ruggedness (M3) is related to the average gradient of an upslope area, and as such is related to the average shear stress exerted by runoff in the contributing area. In addition, the gradient value in the terrain steepness variable included in M1 is nearly identical to the threshold slope value of Prancevic et al. (2014), who used laboratory experiments to examine the transition from water flow to debris flow in steep channels. The authors identified a threshold channel slope of approximately 22°, above which the critical Shields stress for bed failure decreases markedly with increasing channel slope. In this scenario, debris-flow initiation is possible when lower critical Shields stresses are combined with rapid pulses of fine sediment input from hillslopes (Prancevic et al., 2014; Prancevic and Lamb, 2015).

Two measures of wildfire severity that yielded a positive relation between fire severity and debris-flow occurrence are represented in the final models: the average dNBR of all upslope pixels divided by 1000 (M1, M2, and M4), and the proportion of upslope area soils burned at high or moderate severity. The average dNBR in models M1 and M4 is normalized by 1000 to provide a consistent range of values (between 0 and approximately 1) for all coefficients (C_1, C_2, and C_3), and the variables of T, F, and S. Soil burn severity and dNBR are related to one another, as the dNBR serves as the basis for imagery classification and characterization of burn severity (Key and Benson, 2006; Eidenshink et al., 2007). Both metrics reflect the elevated potential for runoff generation and erosion.

Two measures of soil properties were found to exert the greatest influence on post-fire debris-flow occurrence: (1) the KF-Factor, also known as the soil erodibility index of the fine fraction of the soil (M1 and M2), and (2) soil thickness divided by 100 (M3 and M4) (also normalized to provide consistent ranges of coefficient values). The soil KF-Factor reflects the ease at which the fine fraction of the soil is eroded, with higher values of KF reflecting higher erosion potential. Field studies of post-fire erosion have identified the importance of interrill processes

Table 5
Evaluation metrics for the four tested logistic models and regional rainfall–intensity duration thresholds against the test dataset. Regional threshold performance (T_R) was evaluated based on the thresholds listed in Fig. 3.

Training data	Duration (min)	M1	M2	M3	M4	T_R
True	15	584	586	584	587	664
negative	30	568	566	571	574	616
(*TN*)	60	536	536	539	542	650
False	15	105	105	104	107	60
negative	30	102	103	97	100	33
(*FN*)	60	108	108	100	103	58
False	15	30	28	32	27	82
positive	30	34	36	33	28	135
(*FP*)	60	36	36	35	30	90
True	15	96	96	97	94	141
positive	30	99	98	104	101	168
(*TP*)	60	93	93	101	98	143
Threat	15	0.42	0.42	0.42	0.41	0.50
Score	30	0.42	0.41	0.44	0.44	0.50
(*TS*)	60	0.39	0.39	0.43	0.42	0.49
Akaike	15	643.16	647.92	654.5	633.3	-
Information	30	632.68	636.26	634.15	619.12	-
Criterion (*AIC*)	60	642.18	647.06	641.6	627.53	-
Test data	Duration (min)	M1	M2	M3	M4	T_R
True	15	154	152	191	143	348
negative	30	203	202	228	180	340
(*TN*)	60	278	282	321	272	374
False	15	20	21	19	21	22
negative	30	28	28	24	23	36
(*FN*)	60	51	52	51	53	71
False	15	111	113	179	122	130
positive	30	106	107	176	129	138
(*FP*)	60	66	62	99	72	104
True	15	83	82	114	82	107
positive	30	69	69	103	74	93
(*TP*)	60	44	43	48	42	58
Threat	15	0.39	0.38	0.37	0.36	0.41
Score	30	0.34	0.34	0.34	0.33	0.35
(*TS*)	60	0.27	0.27	0.24	0.25	0.25

Table 4
Parameter values, coefficients, and variables for the four models (M1, M2, M3, and M4) analyzed in this study and at rainfall durations of 15, 30, and 60 min.

	M1	M2	M3	M4
β (15, 30, 60)	−3.63, −3.61, −3.21	−3.62, −3.61, −3.22	−3.71, −3.79, −3.46	−3.60, −3.64, −3.30
C_1(15, 30, 60)	0.41, 0.26, 0.17	0.64, 0.42 ,0.27	0.32, 0.21, 0.14	0.51, 0.33, 0.20
X_1R	Proportion of upslope area burned at high or moderate severity with gradients ≥23° * Rainfall accumulation	Average gradient [Sin(θ)] of Upslope area burned at High or Moderate severity * Rainfall accumulation	Ruggedness * Rainfall accumulation	Proportion of upslope area burned with gradients ≥30° * Rainfall accumulation
C_2(15, 30, 60)	0.67, 0.39, 0.20	0.65, 0.38, 0.19	0.33, 0.19, 0.10	0.82, 0.46, 0.24
X_2R	(dNBR/1000) * Rainfall accumulation	(dNBR/1000) * Rainfall accumulation	Proportion of basin burned at high or moderate severity * Rainfall accumulation	(dNBR/1000) * Rainfall accumulation
C_3	0.70, 0.50, 0.220	0.68, 0.49, 0.22	0.47, 0.36, 0.18	0.27, 0.26, 0.13
X_3R	Soil KF-Factor * Rainfall accumulation	Soil KF-Factor * Rainfall accumulation	(Soil thickness/100) * Rainfall accumulation	(Soil thickness/100) * Rainfall accumulation

for both runoff-related sediment transport and debris-flow initiation (Staley et al., 2014; Rengers et al., 2016). Given the relatively low flow velocities and Shields stresses associated with interrill erosion processes, fine particles would constitute a large fraction of the sediment mobilized in these areas. We speculate that soil thickness characterizes sediment availability. Given the coarse resolution of the input soil property dataset (STATSGO, from Schwartz and Alexander, 1995), the direct interpretation of the influence of each of these variables on debris-flow generation requires further investigation. However, the addition of these metrics led to improved model predictions, and therefore these metrics were valuable additions to the final logistic models.

Visual assessment of the sensitivity of each logistic model for all durations revealed that no model was overly sensitive to any single variable. Irrespective of the duration, all analyzed models were most sensitive to rainfall accumulation (*R*, blue line, in Fig. 2). All models, with the exception of M3 at the 15-min duration (where terrain steepness and fire intensity were virtually identical in similarity), proved to be second-most sensitive to the terrain steepness variable (X_1, red line in Fig. 2), and second-most sensitive to fire severity variables (X_2, green line in Fig. 2). All of the final logistic models were least sensitive to changes in soil property values (X_3, brown line in Fig. 2).

5.2. Model evaluation

We evaluated the predictive power of each logistic model by comparing the predictions based on regional rainfall intensity–duration thresholds (Table 2) to the directly calculated intensity–duration thresholds (M1, M2, M3, and M4 in Table 4) at durations of 15, 30, and 60 min using the ROC threat score metric. We evaluated the performance of models at each duration to determine the optimal duration over which debris-flow predictions should be made, and then determined which model performed best at all analyzed durations.

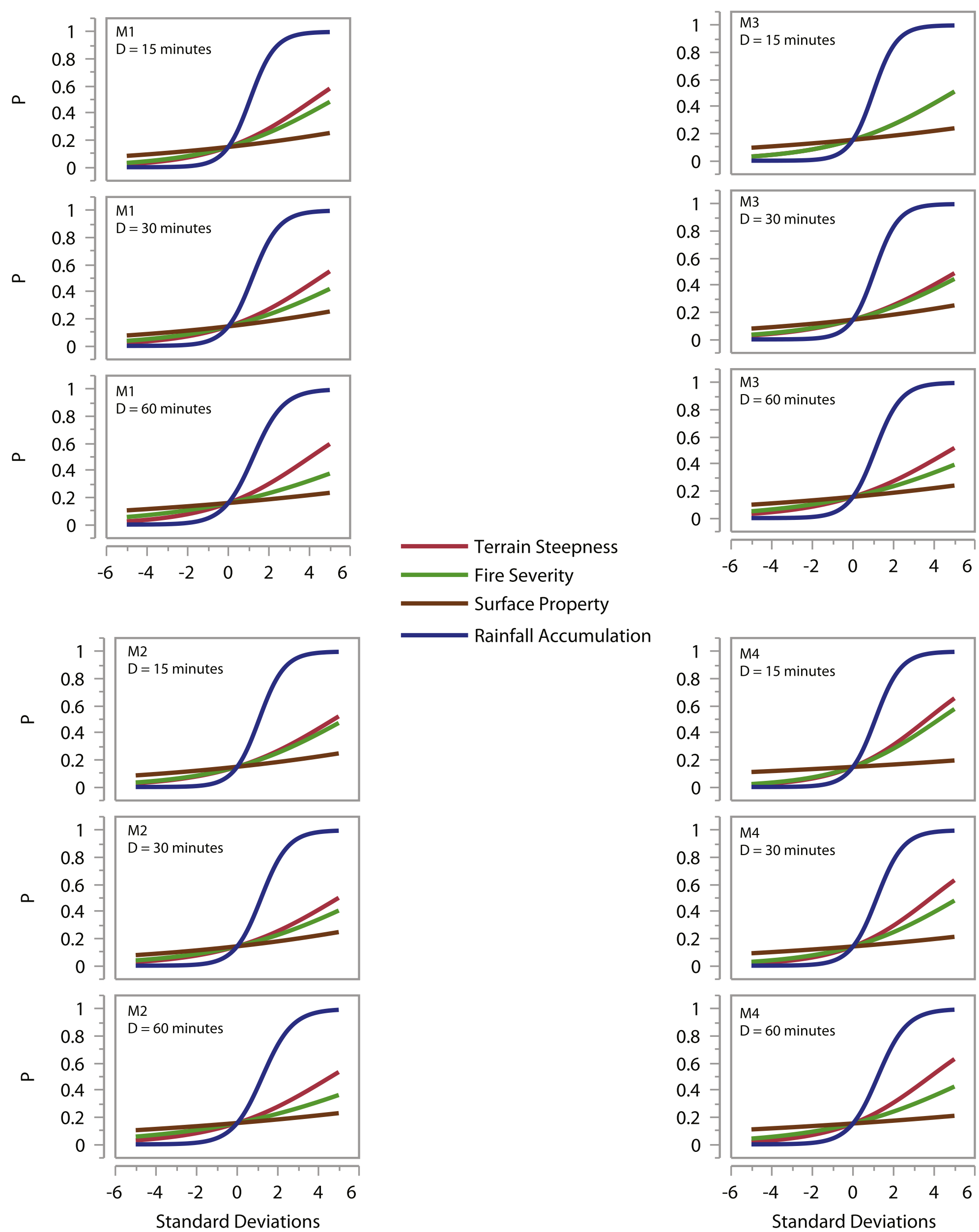

Fig. 2. Sensitivity analysis for the four final logistic models at each analyzed duration. Blue line represents the rainfall accumulation variable (*R*), red line represents the terrain steepness variable (*T*), green line represents the fire severity variable (*F*), and the brown line represents the soil properties variable (*S*). (For interpretation of the references to color in this figure legend, the reader is referred to the web version of this article.)

Overall, 15-min duration thresholds provided the most accurate predictions of post-fire debris-flow generation for all logistic models, as well as the regional thresholds (Table 5). This finding is consistent with field observations of the strong temporal relation between short bursts of high-intensity rainfall and post-fire debris flow initiation (Kean et al., 2011; Staley et al., 2013b). Staley et al. (2013b) evaluated objectively defined rainfall intensity–duration thresholds based on triggering intensities and identified that thresholds based upon 15- and 30-min durations were most accurate. We attribute the decrease of model accuracy with increasing duration as a result of the nature of the storms that produce post-fire debris flows in the western United States. Of the 133 records where post-fire debris-flows were identified in the test dataset, 56 storms were of durations lasting <60 min. These storms tended to be small, fast-moving convective cells, and are not well characterized by intensities measured over durations >30 min.

For all records in the training and test datasets, we compared the model predictions to those of the published regional thresholds (Table 2). For the training dataset, the regional thresholds outperformed all four models at all durations, as evidenced by the threat score values (Table 5). For the test dataset, the predicted thresholds provided similar threat score values when compared to the predictions based on regional intensity–duration thresholds at all durations (Table 5). M1 threat scores were the same as or slightly outperformed all other models and were most similar to the existing regional thresholds for the test dataset.

We also assessed the performance of the modeled thresholds compared to the individual regional thresholds (Fig. 3). For the training dataset (Fig. 3), regional thresholds outperformed modeled thresholds for two of the three threshold regions (Orange and San Diego Counties [OSD] and the San Gabriel, San Bernardino and San Jacinto Mountains

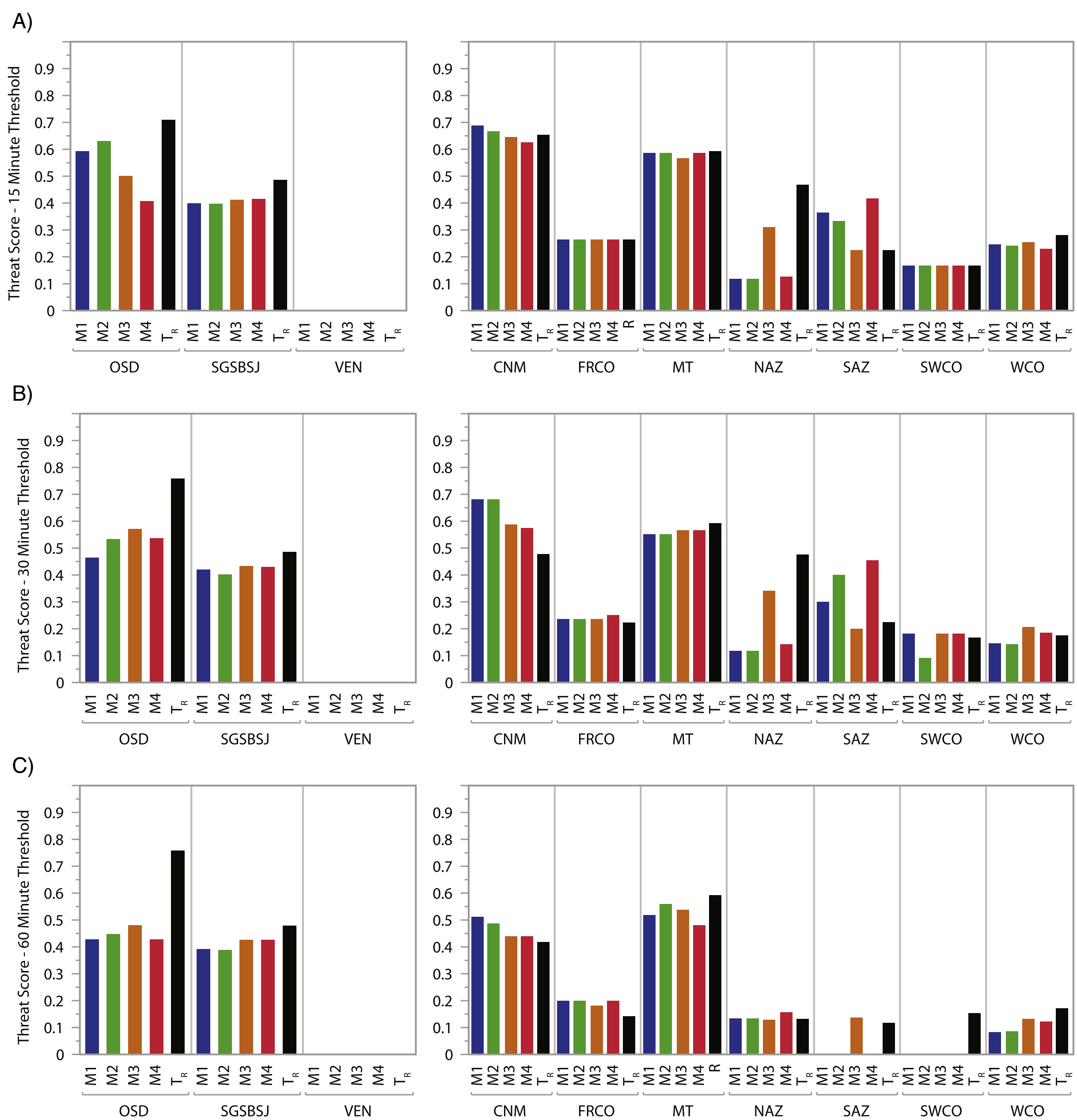

Fig. 3. Comparison of threat scores of all models (M1 in blue, M2 in green, M3 in orange, and M4 in red) and regional thresholds (T_R, in black) for durations of 15 min (A), 30 min (B) and 60 min (C). The Ventura Region (VEN) had no debris-flow events in the updated database, hence a threat score = 0 for M1–M4 and the regional threshold. (For interpretation of the references to color in this figure legend, the reader is referred to the web version of this article.)

[SGSBSJ]) that covered the records in the training dataset. No instances of debris-flow occurrence were included in the dataset for the Ventura (VEN) region; as such, the threat score for all analyzed models and the regional threshold was equal to zero. For the test dataset, modeled thresholds frequently performed at a similar, or slightly improved, degree of accuracy than the individual regional thresholds (Fig. 3). Regional thresholds performed slightly better than all models in Montana (MT) at 30 and 60 min durations, and western Colorado (WCO) at all durations, and markedly better than modeled thresholds in northern Arizona (NAZ) at durations of 15 and 30 min. We attribute the low accuracy of the model predictions in northern Arizona to the extreme magnitude (>10-year recurrence interval) of the debris-flow generating storms (NOAA, 2016). Here, the regional threshold was defined at the lower limit of the rainfall intensities associated with debris-flow occurrence, which resulted in very high threshold intensities (see Table 2). The modeled thresholds, which are much more conservative (i.e. lower threshold intensities), cannot be tested against storms of more modest rainfall intensities. As such, we recommend further model testing in northern Arizona to fully assess the predictive accuracy of the models in this location.

Unlike regional thresholds, which require a great deal of effort to obtain, our modeling represents a fully predictive approach that provides similar levels of accuracy for areas where no historical debris-flow occurrence data are available. Overall, we recommend the use of the M1 logistic model for the spatially explicit prediction of rainfall intensity–duration thresholds in the western United States, as this model provides the most consistent improvement over regional thresholds in the test dataset, and is similar in performance to other models for the training data. We use the results of M1 for the case studies presented in the following sections.

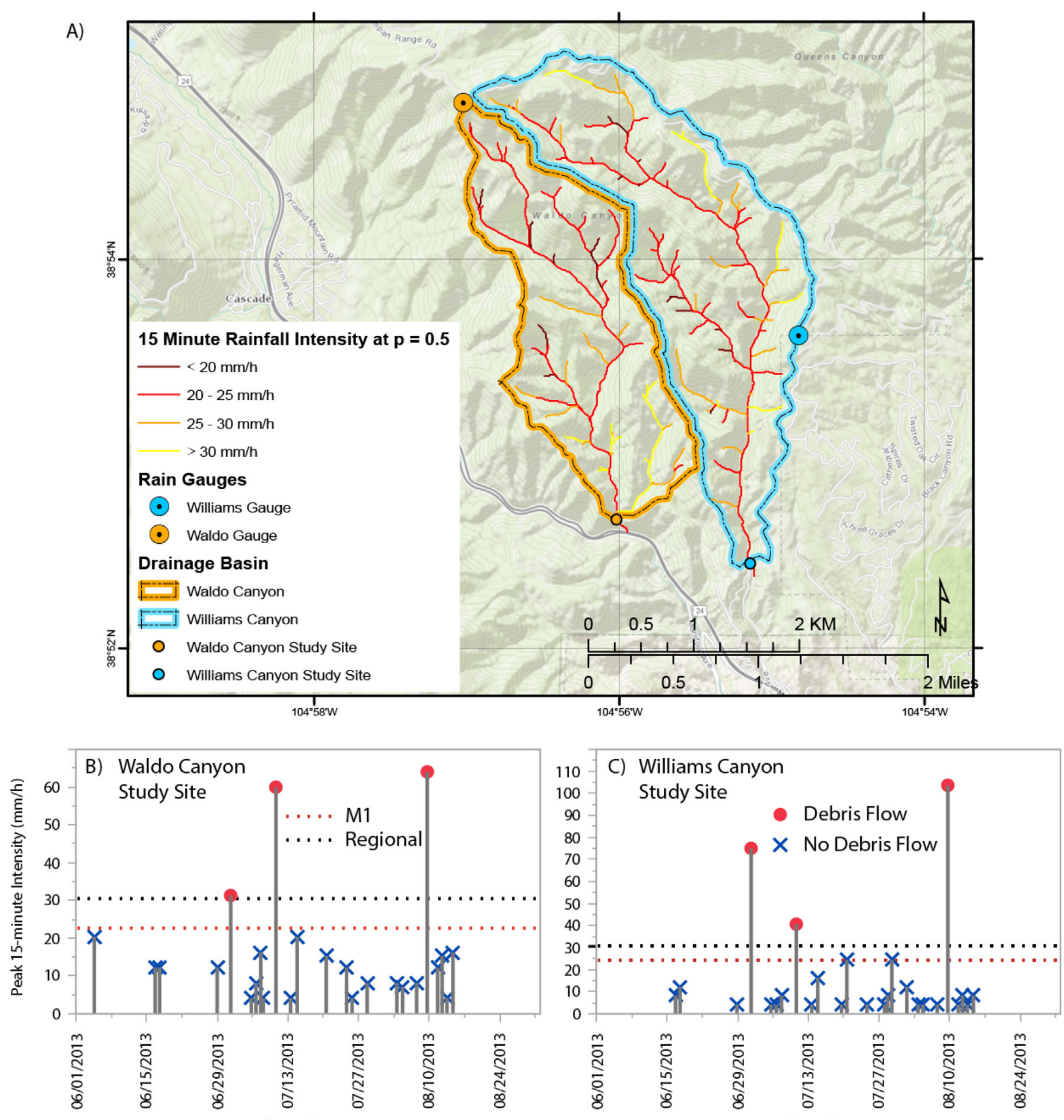

Fig. 4. Results of the geospatial application of M1 15-min rainfall duration to Waldo and Williams Canyons, located in the 2012 Waldo Canyon burn area. A) Map representing the threshold rainfall intensities at which $p = 0.5$. B) Peak rainfall intensities and hydrologic response for individual rainstorms during the summer of 2013 in Waldo Canyon. C) Peak rainfall intensities and hydrologic response for individual rainstorms during the summer of 2013 in Waldo Canyon. In both B) and C) the 15-min threshold calculated by M1 is represented by a red dashed line, while the regional threshold is represented by the dashed black line. Debris-flow producing rainfall intensities are represented by a red dot, while rainfall intensities that did not produce debris flows are represented by a blue X in both B) and C). (For interpretation of the references to color in this figure legend, the reader is referred to the web version of this article.)

5.3. Case study – Waldo and Williams Canyons, Waldo Canyon burn area, Colorado

To demonstrate the ability of the method to resolve spatial variability in rainfall thresholds, we applied the M1 model at the scale of a stream segment (length of channel between tributary junctions) to map the distribution of 15-min rainfall thresholds throughout Waldo and Williams Canyons, which were burned in the 2012 Waldo Canyon fire, Colorado. These canyons produced floods and debris flows on 01 July, 10 July, and 09 August 2013. The final storm resulted in a fatality, and all three storms damaged homes in nearby Manitou Springs, CO, and inundated U.S. Highway 24, a major east-west transportation corridor connecting the City of Colorado Springs to mountain communities to the west. Analysis of the 15-min rainfall thresholds and hydrologic response of Waldo (M1 15-min threshold $= 22.7$ mm h^{-1}) and Williams Canyons (M1 15-min threshold $= 24.4$ mm h^{-1}) revealed thresholds predicted by M1 correctly predicted the three debris-flow producing rainfall intensities, as well as the lack of any hydrologic response to 44 other storms where peak intensities were below the threshold. In addition, the thresholds calculated using M1 were just above the rainfall intensities of storms that occurred in Williams Canyon on 20 July and 29 July 2012, both of which had peak 15-min storm intensities of 24.3 mm h^{-1} ($p = 0.49$) and did not produce debris flows at the basin outlet (Fig. 4C). While the regional threshold also correctly predicted these non-events, the ability of M1 to correctly predict the hydrologic response at a high level of precision suggests a high degree of accuracy and precision when using these methods to predict the hydrologic response of recently burned locations in environments markedly different from those used to develop the model equations.

5.4. Case study – Mullally Canyon, Station burn area, California

We demonstrate potential real-time capabilities of the proposed model by analyzing the temporal evolution of an intense, debris-flow producing rainstorm on 06 February 2010 that damaged 43 homes in La Canada – Flintridge, Calif., downstream from Mullally Canyon (Lin et al., 2010). Fortunately, no fatalities or injuries were a direct result of this event. Although this event was included in the training dataset, it only represents a single record of peak storm intensity. Therefore, the relatively minor influence this storm and location had on the original model calibration, combined with the proximity of installed monitoring equipment, make it ideal for evaluating the near-real-time capability of the proposed methodology. Specifically, we applied the M1 15-min intensity equation to simulate the real-time statistical likelihood values during the rainfall event (Fig. 5) to determine if the proposed methods could be implemented within a near real-time early warning framework.

The storm produced four local peaks in rainfall intensity (2:12 a.m., 3:24 a.m., 5:12 a.m., and 7:20 a.m.). Instrumental monitoring of flow stage at the mouth of the canyon revealed three distinct debris-flow surges (Kean et al., 2012), the first at 3:24 a.m., the second at 5:12 a.m., and the third at 7:20 a.m.. Eyewitness accounts suggest that the second surge overfilled the sediment retention basin, inundating homes and roadways downstream. Real-time likelihood values were below the threshold for the first local peak in rainfall intensity (2:12 a.m., where no debris-flow surge was recorded), and exceeded the M1 15-min intensity-duration threshold for all three of the recorded debris-flow surges (Fig. 5).

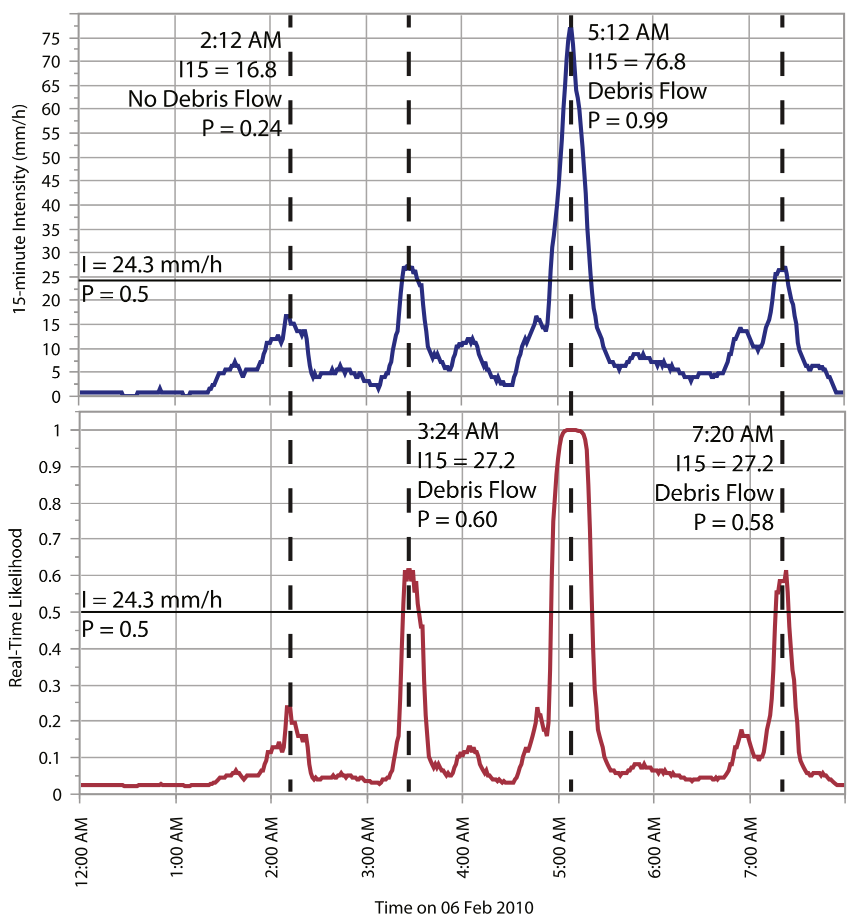

Fig. 5. Real-time 15-min rainfall intensity (top) and M1 statistical likelihood values (bottom) for Mullally Canyon above La Canada – Flintridge, California, where 43 homes were damaged during an intense rainstorm on 06 February 2010. Dashed lines represent local peaks in rainfall intensity. Three separate debris-flow surges were recorded by Kean et al. (2012), the first at 3:24 a.m., the second at 5:12 a.m., and the third at 7:20 a.m.. Statistical likelihood values for all three surges exceeded the M1 15-min intensity duration threshold.

Our results suggest that this method demonstrates potential utility for real-time implementation in an early warning framework. While the USGS/NOAA early warning system accurately issued warnings for this rainstormt, our methods would have also correctly predicted the generation of debris flow for all three surges. It is unlikely that the near real-time predictions of debris-flow likelihood and volume could have led to any actionable decisions that would have prevented the disastrous consequences of any subsequent debris-flow surges. However, the instantaneous nature of the model predictions would have provided real-time estimates of debris-flow likelihood. These estimates, if calculated for multiple watersheds, could have been used for identifying the most likely impacted areas, thereby assisting in the prioritization of locations for emergency response efforts. Although the results of this analysis are promising for early warning, further testing and model calibration should be done prior to incorporation of these methods into any operational warning system.

6. Conclusions

By merging traditional approaches for debris-flow susceptibility mapping with rainfall threshold identification, this paper described a new fully predictive framework for assessing post-fire debris flow hazards using free, readily available geospatial data. Our approach can be used to predict rainfall intensity–duration thresholds for recently burned areas in the western United States where there are no preexisting historical data concerning rainfall rates responsible for post-fire debris-flow generation, as well as map the probability of debris flow in response to design storms. Specifically, the M1 logistic model is recommended for use in the western United States, as it objectively produced better predictions of debris-flow occurrence in both the training and test datasets when compared to the three other logistic models and the existing regional intensity–duration thresholds. The methods presented in this study are applicable for locations situated in recently burned areas for a period of one to two years following wildfire. Additional research, including long-term post-fire monitoring, is needed to better constrain the relation between recovery of the vegetation and soil systems and the reduction of debris-flow susceptibility, and ultimately the increasing rainfall intensity required to generate debris flows in older burn areas. The models presented here are not applicable to unburned areas, or areas where post-fire debris flows are generated from infiltration-related shallow landslides.

The methods presented here permit the expansion of the NOAA/USGS post-fire debris-flow early warning system in new regions of the western United States, as the logistic models provide guidance for the determination of rainfall intensity–duration thresholds for debris-flow generation. Furthermore, the model presented here may be useful for emergency planning purposes, as the site-specific rainfall intensity–duration thresholds can be calculated for individual locations of high importance, such as schools, hospitals and high-value infrastructure. With further model validation and testing, this new model demonstrates a potential for the calculation of real-time debris-flow likelihood values during rainstorms in an early warning framework.

Acknowledgments

This research was made possible with funding from the U.S. Geological Survey Landslide Hazards Program and Multi-Hazards Demonstration Project. The authors are grateful for the field assistance from Joseph Gartner, Kevin Schmidt, Anne-Marie Matherne, Maiana Hanshaw, Robert Leeper, and Octavanio Lucero, and for the rainfall data provided by Pete Wohlgemuth and Terri Hogue. We also would like to acknowledge Sue Cannon for her seminal work defining rainfall intensity–duration thresholds for post-fire debris-flow generation in the western United States, developing probabilistic hazard assessment methods, and establishing the debris-flow early warning system with the National Weather Service in southern California.

References

Akaike, H., 1974. A new look at the statistical model identification. Inst. Electr. Electron. Eng. (IEEE) Trans. Autom. Control 19, 716–723.
Al-Hamdan, O.Z., Pierson, F.B., Nearing, M.A., Williams, C.J., Stone, J.J., Kormos, P.R., Boll, J., Weltz, M.A., 2012. Concentrated flow erodibility for physically based erosion models: temporal variability in disturbed and undisturbed rangelands. Water Resour. Res. 48, W07504.
Balfour, V.N., Doerr, S.H., Robichaud, P.R., 2014. The temporal evolution of wildfire ash and implications for post-fire infiltration. Int. J. Wildland Fire 23, 733–745.
Baum, R.L., Godt, J.W., Savage, W.Z., 2010. Estimating the timing and location of shallow rainfall-induced landslides using a model for transient, unsaturated infiltration. J. Geophys. Res. 115, F03013.
Bodí, M.B., Martin, D.A., Balfour, V.N., Santín, C., Doerr, S.H., Pereira, P., Cerdà, A., Mataix-Solera, J., 2014. Wildland fire ash: production, composition and eco-hydro-geomorphic effects. Earth Sci. Rev. 130, 103–127.
Bovis, M.J., Jakob, M., 1999. The role of debris supply conditions in predicting debris flow activity. Earth Surf. Process. Landf. 24, 1039–1054.
Brunetti, M.T., Peruccacci, S., Rossi, M., Luciani, S., Valigi, D., Guzzetti, F., 2010. Rainfall thresholds for the possible occurrence of landslides in Italy. Nat. Hazards Earth Syst. Sci. 10, 447–458.
Caine, N., 1980. The rainfall intensity: duration control of shallow landslides and debris flows. Geogr. Ann. Ser. A Phys. Geogr. 62, 23–27.
Cannon, S.H., 2001. Debris-flow generation from recently burned watersheds. Environ. Eng. Geosci. 7, 321–341.
Cannon, S.H., DeGraff, J., 2009. The Increasing Wildfire and Post-Fire Debris-Flow Threat in Western USA, and Implications for Consequences of Climate Change. In: Sassa, K., Canuti, P. (Eds.), Landslides – Disaster Risk Reduction. Springer, Berlin Heidelberg (177-190 pp.).
Cannon, S.H., Gartner, J.E., Parrett, C., Parise, M., 2003. Wildfire-related debris-flow generation through episodic progressive sediment-bulking processes, western USA. In: Rickenmann, D., Chen, C.L. (Eds.), Debris-Flow Hazards Mitigation - Mechanics, Prediction, and Assessment, Proceedings of the Third International Conference on Debris-Flow Hazards Mitigation, Davos, Switzerland, 10–12 September 2003. A.A. Balkema, Rotterdam (71-82 pp.).
Cannon, S.H., Gartner, J.E., Wilson, R., Bowers, J., Laber, J., 2008. Storm rainfall conditions for floods and debris flows from recently burned areas in southwestern Colorado and southern California. Geomorphology 96, 250–269.
Cannon, S.H., Gartner, J.E., Rupert, M.G., Michael, J.A., Staley, D.M., Worstell, B.B., 2009. Emergency Assessment of Postfire Debris-flow Hazards for the 2009 Station Fire, San Gabriel Mountains, Southern California. U.S. Geological Survey Open-File Report 2008-1370 (20 pp.).
Cannon, S.H., Gartner, J.E., Rupert, M.G., Michael, J.A., Rea, A.H., Parrett, C., 2010. Predicting the probability and volume of postwildfire debris flows in the intermountain western United States. Geol. Soc. Am. Bull. 122, 127–144.
Cannon, S.H., Boldt, E., Laber, J., Kean, J., Staley, D., 2011. Rainfall intensity–duration thresholds for postfire debris-flow emergency-response planning. Nat. Hazards 59, 209–236.
Carrara, A., Crosta, G., Frattini, P., 2008. Comparing models of debris-flow susceptibility in the alpine environment. Geomorphology 94, 353–378.
Cervi, F., Berti, M., Borgatti, L., Ronchetti, F., Manenti, F., Corsini, A., 2010. Comparing predictive capability of statistical and deterministic methods for landslide susceptibility mapping: a case study in the northern Apennines (Reggio Emilia Province, Italy). Landslides 7, 433–444.
Chawner, W.D., 1935. Alluvial fan flooding: the Montrose, California flood of 1934. Geogr. Rev. 25, 235–263.
DeBano, L.F., 2000. The role of fire and soil heating on water repellency in wildland environments: a review. J. Hydrol. 231–232, 195–206.
DeGraff, J.V., Cannon, S., Gartner, J.E., 2015. The timing of susceptibility to post-fire debris flows in the western USA. Environ. Eng. Geosci. 21, 277–292.
Eaton, E.C., 1935. Flood and erosion control problems and their solution. Proc. Am. Soc. Civ. Eng. 62, 1302–1362.
Ebel, B.A., Moody, J.A., 2013. Rethinking infiltration in wildfire-affected soils. Hydrol. Process. 27, 1510–1514.
Eidenshink, J., Schwind, B., Brewer, K., Zhu, Z.-L., Quayle, B., Howard, S., 2007. A project for monitoring trends in burn severity. J. Assoc. Fire Ecol. 3, 3–21.
Fawcett, T., 2006. An introduction to ROC analysis. Pattern Recogn. Lett. 27, 861–874.
Florsheim, J.L., Keller, E.A., Best, D.W., 1991. Fluvial sediment transport in response to moderate storm flows following chaparral wildfire, Ventura County, southern California. Geol. Soc. Am. Bull. 103, 504–511.
Florsheim, J.L., Chin, A., O'Hirok, L.S., Storesund, R., 2016. Short-term post-wildfire dry-ravel processes in a chaparral fluvial system. Geomorphology 252, 32–39.
Frattini, P., Crosta, G., Sosio, R., 2009. Approaches for defining thresholds and return periods for rainfall-triggered shallow landslides. Hydrol. Process. 23, 1444–1460.
Friedman, E.Q., Santi, P.M., 2014. Debris-flow hazard assessment and validation following the Medano Fire, Great Sand Dunes National Park and Preserve, Colorado. Landslides 11, 1093–1113.
Gabet, E.J., 2003a. Post-fire thin debris flows: sediment transport and numerical modelling. Earth Surf. Process. Landf. 28, 1341–1348.
Gabet, E.J., 2003b. Sediment detachment by rain power. Water Resour. Res. 39, ESG 1-1–ESG 1-12.
Gabet, E.J., 2003c. Sediment transport by dry ravel. J. Geophys. Res. 108, 2049.
Gartner, J., Cannon, S., Santi, P., Dewolfe, V., 2008. Empirical models to predict the volumes of debris flows generated by recently burned basins in the western U.S. Geomorphology 96, 339–354.
Gartner, J.E., Cannon, S.H., Santi, P.M., 2014. Empirical models for predicting volumes of sediment deposited by debris flows and sediment-laden floods in the transverse ranges of southern California. Eng. Geol. 176, 45–56.
Giovannini, G., Lucchesi, S., 1983. Effect of fire on hydrophobic and cementing substances of soil aggregates. Soil Sci. 136, 231–236.

Giovannini, G., Lucchesi, S., Giachetti, M., 1987. The natural evolution of a burned soil: a three-year investigation. Soil Sci. 143, 220–226.
Godt, J.W., McKenna, J.P., 2008. Numerical Modeling of Rainfall Thresholds for Shallow Landsliding in the Seattle, Washington Area. In: Baum, R.L., Godt, J.W., Highland, L.M. (Eds.), Landslides and Engineering Geology of the Seattle. Geological Society of America Reviews in Engineering Geology, Washington Area (121-135 pp.).
Godt, J.W., Baum, R.L., Chleborad, A.F., 2006. Rainfall characteristics for shallow landsliding in Seattle, Washington, USA. Earth Surf. Process. Landf. 31, 97–110.
Godt, J.W., Baum, R.L., Savage, W.Z., Salciarini, D., Schulz, W.H., Harp, E.L., 2008. Transient deterministic shallow landslide modeling: requirements for susceptibility and hazard assessments in a GIS framework. Eng. Geol. 102, 214–226.
Guzzetti, F., Peruccacci, S., Rossi, M., Stark, C.P., 2007. Rainfall thresholds for the initiation of landslides in central and southern Europe. Meteorog. Atmos. Phys. 98, 239–267.
Guzzetti, F., Peruccacci, S., Rossi, M., Stark, C.P., 2008. The rainfall intensity–duration control of shallow landslides and debris flows: an update. Landslides 5, 3–17.
Hamilton, E.L., Horton, J.S., Rowe, P.B., Reimann, L.F., 1954. Fire-flood Sequences on the San Dimas Experimental Forest. U.S. Department of Agriculture, Forest Service, California Forest and Range Experiment, Technical Paper 6 (29 pp.).
Hosmer, D.W., Lemeshow, S., Sturdivant, R.X., 2000. Applied Logistic Regression. John Wiley and Sons, Inc., New York.
Kean, J.W., Staley, D.M., 2011. Direct Measurements of the Hydrologic Conditions Leading up to and During Post-fire Debris Flow in Southern California, USA. In: Genevois, R., Hamilton, D.L., Prestininzi, A. (Eds.), Proceedings of the Fifth International Conference on Debris Flow Hazards Mitigation/Mechanics, Prediction, and Assessment, Padua, Italy, June 7–11, 2011. Italian Journal of Engineering Geology and Environment–Book: Casa Editrice Universita La Sapienza, Rome, Italy, pp. 685–694.
Kean, J.W., Staley, D.M., Cannon, S.H., 2011. In situ measurements of post-fire debris flows in southern California: comparisons of the timing and magnitude of 24 debris-flow events with rainfall and soil moisture conditions. J. Geophys. Res. 116, F04019.
Kean, J.W., Staley, D.M., Leeper, R.J., Schmidt, K.M., 2012. A low-cost method to measure the timing of post-fire flash floods and debris flows relative to rainfall. Water Resour. Res. 48, W05516.
Kean, J.W., McCoy, S.W., Tucker, G.E., Staley, D.M., Coe, J.A., 2013. Runoff-generated debris flows: observations and modeling of surge initiation, magnitude, and frequency. J. Geophys. Res. Earth Surf. 2013JF002796.
Key, C.H., Benson, N.C., 2006. Landscape Assessment (LA) Sampling and Analysis Methods. USDA Forest Service - General Technical Report RMRS-GTR(164 RMRS-GTR), pp. LA-1–LA-51.
Kinnell, P.I.A., 2005. Raindrop-impact-induced erosion processes and prediction: a review. Hydrol. Process. 19, 2815–2844.
Lamb, M.P., Scheingross, J.S., Amidon, W.H., Swanson, E., Limaye, A., 2011. A model for fire-induced sediment yield by dry ravel in steep landscapes. J. Geophys. Res. 116, F03006.
Lamb, M.P., Levina, M., DiBiase, R.A., Fuller, B.M., 2013. Sediment storage by vegetation in steep bedrock landscapes: theory, experiments, and implications for postfire sediment yield. J. Geophys. Res. Earth Surf. 118, 1147–1160.
Larsen, I.J., MacDonald, L.H., Brown, E., Rough, D., Welsh, M.J., Pietraszek, J.H., Libohova, Z., de Dios Benavides-Solorio, J., Schaffrath, K., 2009. Causes of post-fire runoff and erosion: water repellency, cover, or soil sealing? Soil Sci. Soc. Am. J. 73, 1393–1407.
Letey, J., 2001. Causes and consequences of fire-induced soil water repellency. Hydrol. Process. 15, 2867–2875.
Lin, R.G., Kim, V., Vives, R., 2010. 'Niagara' of Mud Hits Homes; Dozens of Houses in La Canada Flintridge are Damaged or Destroyed in Storm that Defied Forecast. Los Angeles Times (7 February 2010, A.1).
Martin, D.A., Moody, J.A., 2001. Comparison of soil infiltration rates in burned and unburned mountainous watersheds. Hydrol. Process. 15, 2893–2903.
Meyer, G.A., Wells, S.G., 1997. Fire-related sedimentation events on alluvial fans, Yellowstone National Park, U.S.A. J. Sediment. Res. 67, 776–791.
Moody, J.A., Ebel, B.A., 2012. Hyper-dry conditions provide new insights into the cause of extreme floods after wildfire. Catena 93, 58–63.
Moody, J.A., Ebel, B.A., 2014. Infiltration and runoff generation processes in fire-affected soils. Hydrol. Process. 28, 3432–3453.
Moody, J.A., Martin, D.A., 2001. Post-fire, rainfall intensity–peak discharge relations for three mountainous watersheds in the western USA. Hydrol. Process. 15, 2981–2993.
Moody, J.A., Smith, J.D., Ragan, B.W., 2005. Critical shear stress for erosion of cohesive soils subjected to temperatures typical of wildfires. J. Geophys. Res. Earth Surf. 110, F01004.
Moody, J.A., Shakesby, R.A., Robichaud, P.R., Cannon, S.H., Martin, D.A., 2013. Current research issues related to post-wildfire runoff and erosion processes. Earth Sci. Rev. 122, 10–37.
Negri, J.A., 2016 Evaluation and Validation of Multiple Predictive Models Applied to Post-Wildfire Debris-Flow Hazard Prediction. Unpublished M.Sc. Thesis, Colorado School of Mines, Department of Geology, 94 pp.
NOAA, 2005. NOAA and USGS to Conduct Pilot Project for Flash Flood and Debris Flow Warning Systems in Southern California; Improved Capability will Help Save Lives, Minimize Property Damage and Loss, News Release NOAA05-116: 9 September 2005.
NOAA, 2016. National oceanic and atmospheric administration hydrometeorological designs study center precipitation frequency data server (PFDS). http://hdsc.nws.noaa.gov/hdsc/pfds/index.html (Accessed August 30, 2016).
Noske, P.J., Lane, P.N.J., Nyman, P., Sheridan, G.J., 2016. Effects of aridity in controlling the magnitude of runoff and erosion after wildfire. Water Resour. Res. 2015WR017611.
Nyman, P., Sheridan, G.J., Smith, H.G., Lane, P.N.J., 2011. Evidence of debris flow occurrence after wildfire in upland catchments of south-east Australia. Geomorphology 125, 383–401.
Nyman, P., Sheridan, G.J., Moody, J.A., Smith, H.G., Noske, P.J., Lane, P.N.J., 2013. Sediment availability on burned hillslopes. J. Geophys. Res. Earth Surf. 118, 2451–2467.
Nyman, P., Smith, H.G., Sherwin, C.B., Langhans, C., Lane, P.N.J., Sheridan, G.J., 2015. Predicting sediment delivery from debris flows after wildfire. Geomorphology 250, 173–186.
Parise, M., Cannon, S., 2012. Wildfire impacts on the processes that generate debris flows in burned watersheds. Nat. Hazards 61, 217–227.
Parrett, C., 1987. Fire-related debris flows in the Beaver Creek Drainage, Lewis and Clark County, Montana. U. S. Geol. Surv. Water Supply Pap. 2330, 57–67.
Prancevic, J.P., Lamb, M.P., 2015. Particle friction angles in steep mountain channels. J. Geophys. Res. Earth Surf. 120, 242–259.
Prancevic, J.P., Lamb, M.P., Fuller, B.M., 2014. Incipient sediment motion across the river to debris-flow transition. Geology 42 (3), 191–194.
Rengers, F.K., Tucker, G.E., Moody, J.A., Ebel, B.A., 2016. Illuminating wildfire erosion and deposition patterns with repeat terrestrial lidar. J. Geophys. Res. Earth Surf. 2015JF003600.
Rowe, P.B., Countryman, C.M., Storey, H.C., 1949. Probable Peak Discharge and Erosion Rates from Southern California Watersheds as Influenced by Fire. USDA Forest Service, California Forest and Range Experiment Station (Berkeley, CA) Report (305 pp.).
Rupert, M.G., Cannon, S.H., Gartner, J.E., Michael, J.A., Helsel, D.R., 2008. Using Logistic Regression to Predict the Probability of Debris Flows in Areas Burned by Wildfires, Southern California, 2003–2006. U.S. Geological Survey Open-File Report 2008-1370 (16 pp.).
Santi, P., Dewolfe, V., Higgins, J., Cannon, S., Gartner, J., 2008. Sources of debris flow material in burned areas. Geomorphology 96, 310–321.
Schaefer, J.T., 1990. The critical success index as an indicator of warning skill. Weather Forecast. 5, 570.
Schmidt, K.M., Hanshaw, M.N., Howle, J.F., Kean, J.W., Staley, D.M., Stock, J.D., Bawden, G.W., 2011. Hydrologic Conditions and Terrestrial Laser Scanning of Post-fire Debris Flows in the San Gabriel Mountains, CA, USA. In: Genevois, R., Hamilton, D.L., Prestininzi, A. (Eds.), Proceedings of the Fifth International Conference on Debris Flow Hazards Mitigation/Mechanics, Prediction, and Assessment, Padua, Italy, June 7–11, 2011. Italian Journal of Engineering Geology and Environment–Book: Casa Editrice Universita La Sapienza, Rome, Italy, pp. 583–593.
Schumm, S.A., 1980. Some Applications of the Concept of Geomorphic Thresholds. In: Coats, D., Vitek, J.D. (Eds.), Thresholds in Geomorphology. Allen and Unwin, Ltd., London (473–486 pp.).
Schwartz, G.E., Alexander, R.B., 1995. Soils Data for the Conterminous United States Derived from the NRCS State Soil Geographic (STATSGO) Database. U.S. Geological Survey Open-File Report 95-449 (accessed July 2013 at http://water.usgs.gov/lookup/getspatial?/ussoils).
Shakesby, R., Doerr, S., 2006. Wildfire as a hydrological and geomorphological agent. Earth Sci. Rev. 74, 269–307.
Smith, H.G., Sheridan, G.J., Nyman, P., Child, D.P., Lane, P.N.J., Hotchkis, M.A.C., Jacobsen, G.E., 2012. Quantifying sources of fine sediment supplied to post-fire debris flows using fallout radionuclide tracers. Geomorphology 139-140, 403–415.
Staley, D.M., 2014. Emergency Assessment of Post-fire Debris-flow Hazards for the 2013 Springs Fire, Ventura County, California. U.S. Geological Survey Open-File Report 2014–1001 (10 pp.).
Staley, D.M., Gartner, J.E., Smoczyk, G.M., Reeves, R.R., 2013a. Emergency Assessment of Post-fire Debris-flow Hazards for the 2013 Mountain Fire, Southern California. U.S. Geological Survey Open-File Report 2013–1249 (13 pp.).
Staley, D.M., Kean, J.W., Cannon, S.H., Schmidt, K.M., Laber, J.L., 2013b. Objective definition of rainfall intensity–duration thresholds for the initiation of post-fire debris flows in southern California. Landslides 10, 547–562.
Staley, D.M., Smoczyk, G.M., Reeves, R.R., 2013c. Emergency Assessment of Post-fire Debris-flow Hazards for the 2013 Powerhouse Fire, Southern California. U.S. Geological Survey Open-File Report 2013–1248 (13 pp.).
Staley, D.M., Wasklewicz, T.A., Kean, J.W., 2014. Characterizing the primary material sources and dominant erosional processes for post-fire debris-flow initiation in a headwater basin using multi-temporal terrestrial laser scanning data. Geomorphology 214, 324–338.
Staley, D.M., Gartner, J.E., Kean, J.W., 2015. Objective Definition of Rainfall Intensity-duration Thresholds for Post-fire Flash Floods and Debris Flows in the Area Burned by the Waldo Canyon Fire, Colorado, USA. In: Lollino, G., Giordan, D., Crosta, G.B., Corominas, J., Azzam, R., Wasowski, J., Sciarra, N. (Eds.), Engineering Geology for Society and Territory vol. 2. Springer International Publishing (621-624 pp.).
Staley, D.M., Negri, J.A., Kean, J.W., Laber, J.L., Tillery, A.C., Youberg, A.M., 2016. Updated Logistic Regression Equations for the Calculation of Post-Fire Debris-Flow Likelihood in the Western U.S. Geological Survey Open-File Report 2016-1106 (20 pp.).
Swets, J.A., 1988. Measuring the accuracy of diagnostic systems. Science 240, 1285–1293.
Tillery, A.C., Matherne, A.M., Verdin, K.L., 2012. Estimated Probability of Postwildfire Debris Flows in the 2012 Whitewater–Baldy Fire Burn Area, Southwestern New Mexico. U.S. Geological Survey Open-File Report 2012–1188 (11 pp.).
USGS, 2005. NOAA-USGS Debris-Flow Warning System - Final Report. U.S. Geol. Surv. Circ. 1283 (47 pp.).
USGS, 2015. United States Geological Survey, The National Map, 3D Elevation Program. http://nationalmap.gov/3dep_prodserv.html (Accessed 30 August 2016).
USGS, 2016. Emergency Assessment of Post-Fire Debris-Flow Hazards. United States Geological Survey (http://landslides.usgs.gov/hazards/postfire_debrisflow/. Accessed 02 May 2016).
Verdin, K.L., Dupree, J.A., Elliot, J.G., 2012. Probability and Volume of Potential Postwildfire Debris Flows in the 2012 Waldo Canyon Burn Area near Colorado Springs, Colorado. U.S. Geological Survey Open File Report: 2012-1158 (8 pp.).
Wagenbrenner, J.W., Robichaud, P.R., Elliot, W.J., 2010. Rill erosion in natural and disturbed forests: 2. Modeling approaches. Water Resour. Res. 46 (10), W10507.
Wells, W.G., 1987. The effects of fire on the generation of debris flows in southern California. Rev. Eng. Geol. 7, 105–114.
Westerling, A.L., Hidalgo, H.G., Cayan, D.R., Swetnam, T.W., 2006. Warming and earlier spring increase Western U.S. forest wildfire activity. Science 313, 40–943.
Youberg, A., 2014 Modern and ancient debris flows in Arizona. Unpublished Ph.D. Thesis, University of Arizona, Department of Hydrology and Water Resources, 235 pp.